J. Phys. B: At. Mol. Opt. Phys. **32** (1999) 2077–2088. Printed in the UK PII: S0953-4075(99)97770-2

C K-shell absorption and single-hole ionization in the CO molecule in the vicinity of the shape resonance

A A Pavlychev

Institute of Physics, St Petersburg University, St Petersburg, 198904, Russia

Received 22 September 1998, in final form 9 February 1999

Abstract. Inelastic scattering of the primary photoelectron by valence electrons is found to be important in C K-shell photoexcitation of CO. Within the framework of the optical potential concept and the quasi-atomic model, the performed calculations of C K photoexcitation in CO have shown that the photoelectron–valence electron (PEVE) correlations lead to (a) the decrease of the single-hole ionization cross section in comparison with the absorption cross section right above the photoelectron inelastic threshold, (b) an anomalous spectral dependence of both cross sections at the threshold (≈ 302 eV) and (c) an upward shift (≈ 2.3 eV) of the shape resonance. A comparison of the theoretical and experimental (Köppe *et al* 1996 *Chem. Phys. Lett*. **260** 223) C K-shell absorption and single-hole ionization spectra gives evidence of the PEVE correlations. The importance of higher-lying molecular metastable states in C K-shell photoexcitation of CO is shown.

1. Introduction

Shape resonance phenomena in inner-shell absorption and ionization spectra of molecular species have recently received increasing attention [1–8]. The single-electron approximation lying at the heart of numerous shape resonance descriptions gives reasonable agreement with experimental x-ray absorption cross sections (see, e.g., [9–11]). However, it is not clear to what extent this approximation is valid. The recent experimental studies of C K-shell photoexcitation [5] have demonstrated the existence of a deep gap at 301–303 eV in the single-hole ionization $\sigma^{+}_{\mathrm{C\,1s}}(\omega)$ cross section of CO and the disappearance of the shape resonances in $\sigma^{+}_{\mathrm{C\,1s}}(\omega)$ clearly identifiable in the absorption $\sigma^{\mathrm{a}}_{\mathrm{C\,1s}}(\omega)$ cross section of C_2H_n for $n = 4, 6$ [7]. This unexpected spectral behaviour, not predicted by a one-electron description, allows us to assume a noticeable assistance of valence electrons in C K-shell photoexcitation. The autoionization of doubly excited C $1s^{-1}Val^{-1}\pi^{*1}Ryd^{1}$ states into the C $1s^{-1}$ continuum is taken in the work [5] as a probable candidate to rationalize it. In the present study another process, direct knock-out (DKO) of valence electrons by the primary photoelectron, is regarded as a plausible cause to help elucidate this spectral dependence.

The DKO process responsible for inelastic scattering of the photoelectron by outer electrons and their emission and excitation [12] brings correlations to the behaviour of the photoelectron and valence electrons (PEVE). In isolated atoms the DKO effect on inner-shell ionization is not significant in comparison with that initiated by vacancy creation. In most details the DKO effect is studied on the giant resonance in Xe and Ba above the 4d ionization threshold, for which the 5p and 6s orbitals are regarded as outer shells [13, 14]. Amusia *et al*

0953-4075/99/092077+12$19.50

[13, 14] have demonstrated the decrease of the single-ionization cross section right above the double-ionization threshold:

$$\sigma^{+}(\omega) \approx \sigma^{\mathrm{a}}(\omega) \exp(-2 \operatorname{Im} \Delta) \tag{1}$$

where ω is the photon frequency and $\Delta(E)$ is the phase shift due to the scattering of the photoelectron with kinetic energy E on the polarization potential, the imaginary part of which is zero below the double-ionization threshold. At the transition to inner-shell excitations in polyatomic aggregates, two reasons attract our attention to the DKO process. Firstly, the integral coupling of the primary photoelectron with the extended outer subsystem becomes much more effective and the probability of the subsystem being excited by the photoelectron impact magnifies sharply. As a result the σ^{a} and σ^{+} cross sections can differ dramatically. Secondly, shape resonances originating from intramolecular interference are expected to be a sensitive probe of the phase shift Δ dependent on the polarization potential.

The influence of photoelectron energy losses on x-ray absorption fine structure of polyatomic aggregates was considered in [15, 16], but the DKO process has not been thoroughly studied in these papers. This motivated the development of the quasi-atomic (QA) approach to the DKO process and the model calculations of its effect on the spectral dependence of absorption and single-hole ionization given in section 2. The use of an optical molecular potential and the resemblance of DKO of valence shells to molecular electron impact excitations are the key points in understanding the DKO effect on inner-shell excitations. The relations obtained are applicable for excitations localized on atoms with upper shells not contributing essentially to high occupied molecular orbitals (MO) of a compound. To evaluate the DKO effect in practice, the calculated spectral dependence of C K-shell absorption and single-hole ionization of CO is examined (section 3.1) and compared (section 3.2) with the experimental spectra.

2. DKO effect

X-ray absorption and ionization in polyatomic systems are described as atomic processes, the spectral and angular dependences of which are modified by the surroundings [2, 17, 18]. In the framework of the QA model single core-hole ionization with excitation and double ionization can be approximately divided into atomic and extra-atomic parts attributed to the core-ionized atom and its surroundings. This partition is certainly allowed under the assumption that the orbitals of the core-ionized atom do not play an essential role in the creation of high occupied molecular orbitals. The extra-atomic part of the DKO process is illustrated in figure 1 with the help of the quasi-atomic many-body theory diagrams [12–14, 19]. In contrast to the atomic DKO process [12–14], the vacancies $n_0 l_0^{-1}$ and Val^{-1} are now localized in different subsystems: $n_0 l_0 \in$ ionized core atom and $\mathrm{Val} \in$ surroundings. The different localization of the electron–hole pairs makes it possible to assign the diagrams with extrinsic photoelectron losses due to transfer of photoelectron kinetic energy to the surroundings.

Let us consider changes in initial (pre-scattered) photoelectron flux through a sphere of radius R around the absorber [17, 18]. They are determined by the electron-optical properties of the surroundings. At R close to the radius b of the atomic core, the changes in an $l\Gamma$ channel are equal to

$$\mathrm{Re}\left[(\mathbf{1} + \boldsymbol{BS})(\mathbf{1} - \boldsymbol{BS})^{-1}\right]_{l\Gamma l\Gamma} = M^{\mathrm{a}}_{l\Gamma}(E). \tag{2}$$

They give the variation of the spectral distribution of oscillator strengths for an $n_0 l_0 \rightarrow El\Gamma$ transition due to the surroundings effect. Outside the molecular region at $R \geqslant R_{\mathrm{mol}}$ (i.e. near a detector) the changes

$$\Sigma_{l'} \left|\boldsymbol{T}(\mathbf{1} - \boldsymbol{BS})^{-1}\right|^2_{l\Gamma, l'\Gamma} = M^{+}_{l\Gamma}(E) \tag{3}$$

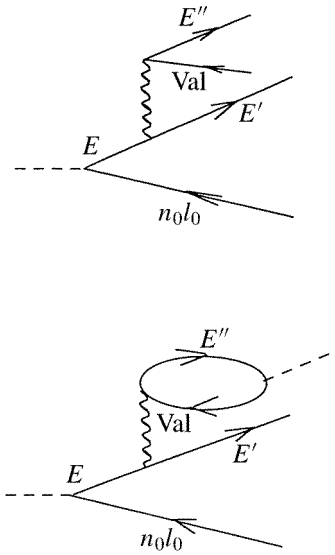

Figure 1. The quasi-atomic diagrams responsible for the correlations in the behaviour of the primary photoelectron and valence electrons.

describe the spectral dependence of the single-hole ionization. $\boldsymbol{B} = \{B_{ll'\Gamma}\}$ and $\boldsymbol{T} = \{T_{ll'\Gamma}\}$ are the reflection and transmission matrices which collect all information on electron-optical properties of the surroundings, Γ is an irreducible representation of the point group of the core-ionized state, l and l' are photoelectron orbital momenta before and after interaction with the anisotropic surroundings and $\boldsymbol{S}$ is the scattering matrix of the absorber. Approximately $M^{\mathrm{a}/+}_{l\Gamma}(E) \approx \sigma^{\mathrm{a}/+}_{\mathrm{core}\to l\Gamma}(E)\big/\sigma^{\mathrm{a}/+}_{\mathrm{core}\to l,\mathrm{atom}}(E)$ where $\sigma^{\mathrm{a}/+}_{\mathrm{core}\to l,\mathrm{atom}}$ is regarded as the partial cross section of absorption/ionization in an isolated absorber: $\boldsymbol{B} \equiv \boldsymbol{0}$ and $\boldsymbol{T} \equiv \boldsymbol{1}$. The DKO process in a free absorbing atom is considered to be insignificant: $\sigma^{\mathrm{a}}_{\mathrm{core}\to l,\mathrm{atom}} = \sigma^{+}_{\mathrm{core}\to l,\mathrm{atom}}$.

Equation (2) shows that the spectral changes in x-ray absorption due to the surroundings are entirely determined by the $B_{ll'\Gamma}$ amplitudes of waves reflected (back scattered) from the surroundings, whereas the changes in photoelectron emission (equation (3)) depend in addition on the $T_{ll'\Gamma}$ amplitudes of waves transmitted through the surroundings. Without inelastic losses $|\boldsymbol{B}(E)|^2 + |\boldsymbol{T}(E)|^2 = 1$, the photoelectron current is independent of R and $M^{\mathrm{a}}_{l\Gamma}(E) = M^{+}_{l\Gamma}(E)$. But if the losses are taken into account this current becomes R dependent and the spectral behaviour of absorption and single-ionization cross sections differ from one another.

How do the extrinsic losses influence spectral properties of absorption and single-hole ionization? To answer the question we introduce dissipation of the photoelectron current by adding an imaginary part to the potential of the surroundings [20]

$$W^{\mathrm{opt}}(E, r) = W(E, r) - \mathrm{i}U(E, r) \tag{4}$$

(positive U values refer to dissipation of the photoelectron current) and consider the relevant changes in the $\boldsymbol{B}$ and $\boldsymbol{T}$ matrices and, then, in the $M^{\mathrm{a}}_{l\Gamma}(E)$ and $M^{+}_{l\Gamma}(E)$ functions. By utilizing the zeroth-range potential approximation [21] to the environment atoms and by neglecting the hybridization of the initial atomic partial l with other l' waves, relationships between the spectral dependences and the optical potential (4) can be simplified. The ll'-hybridization mainly controls the angular [2] but not the spectral dependence of the photoelectron yield.

The $\boldsymbol{B}_{ll\Gamma}(E)$ and $\boldsymbol{T}_{ll\Gamma}(E)$ amplitudes obey the equations

$$2\mathrm{i}k\frac{\partial}{\partial r}B_{ll\Gamma}(E,r) = W^{\mathrm{opt}}\left[\varphi^{+} + B_{ll\Gamma}(E,r)\varphi^{-}\right]^{2} \tag{5}$$

$$2\mathrm{i}k\frac{\partial}{\partial r}T_{ll\Gamma}(E,r) = W^{\mathrm{opt}}T_{ll\Gamma}(E,r)\varphi^{-}\left[\varphi^{+} + B_{ll\Gamma}(E,r)\varphi^{-}\right]. \tag{6}$$

Integrating them with the boundary conditions of $B_{ll\Gamma}(E, R_{\mathrm{mol}}) = 0$ and $T_{ll\Gamma}(b) = 1$, the amplitudes can be found analytically. φ^{+} and φ^{-} are outgoing and incoming atomic wavefunctions, respectively, with asymptotes $\sim \exp[\pm\mathrm{i}(kr - \pi l/2)]$ where k is a photoelectron wavenumber. Coulomb attraction outside of the molecular sphere is neglected here. In the approximations the spectral behaviour of the photoprocesses is dependent on the radial distribution of surrounding scatters, their scattering length and the function of energy losses.

For the surroundings consistent in a single coordination sphere of R radius the solution of equation (5) gives

$$|B| = \left[1 + z^{2}Z\right]^{-1/2} \qquad \text{and} \qquad \arg B = 2kR + \phi = 2kR + \phi^{\mathrm{el}} + \beta = \arg B^{\mathrm{a}} + \beta \tag{7}$$

where

$$Z = \frac{1+x}{1+y^{2}} \qquad \beta = \tan^{-1}(2z + y) - \tan^{-1}(2z) - \tan^{-1}(y)$$

$$x = \frac{U}{k} \qquad z = \frac{k}{W} \qquad y = xz.$$

Hereafter spectral dependences of magnitudes found without an imaginary part in the potential (4) are denoted by the superscript 0 and the subscripts $ll\Gamma$ are omitted. The Z and β functions characterize the coupling of elastic and inelastic channels. $Z \to 1$, $\beta \to 0$ and $B(k) \to B^{0}(k)$ in the limiting case $U \to 0$. From equation (7), it follows that

$$|B| \geqslant \left|B^{0}\right| \qquad \text{if} \quad Z \leqslant 1 \tag{8}$$

and

$$\arg B \leqslant \arg B^{0} \qquad \text{if} \quad W \geqslant 0. \tag{9}$$

The solution of (6) is more complicated as it depends on the solution of equation (5). We mark only the appearance of an exponentially damping factor

$$|T| \sim \left|T^{0}\right|\mathrm{e}^{-x/2} \tag{10}$$

which gives the main change in photoelectron transmission. The arg T is not discussed because it influences the angular but not the spectral distribution of the photoelectrons.

In non-metals the DKO process arises above the single-ionization threshold E_{nl} and provokes irregular behaviour of both the cross sections at $\omega_{\varepsilon} \approx E_{nl} + \varepsilon$, where ε is the energy of the photoelectron inelastic threshold (IT). This IT feature is related to the Wigner–Baz effect [22, 23] describing the changes in the elastic scattering amplitude near ITs.

As an illustration, typical spectral dependences of $|B|$ and absorption and single-hole ionization cross sections computed with the help of equations (2)–(10) for the model $W^{\mathrm{opt}}(E, \boldsymbol{R})$ potential are plotted in figure 2. Figures 2(*a*) and (*b*) show changes in $|B|(E)$ and $\sigma^{\mathrm{a}}(E)$ due to the increase of the imaginary part in the optical potential $(0, U_1 < U_2 < U_3)$ with $\varepsilon = 0$. The real part is invariant and it is chosen to model two resonance features in figure 2(*b*). Their monotonic blue shift and non-monotonic changes of their maxima with increasing U are seen. Figures 2(*c*) and (*d*) show spectral dependences of σ^{a} and σ^{+} at IT. The transition from the bold curve to other curves in figure 2(*b*) in the ε vicinity describes the irregular IT behaviour as $U(E) = U$ if $E \geqslant \varepsilon$ and $U(E) = 0$ if $E < \varepsilon$. The breaks in figures 2(*c*) and (*d*) originate first of all from the additional phase shift β. They are indicated

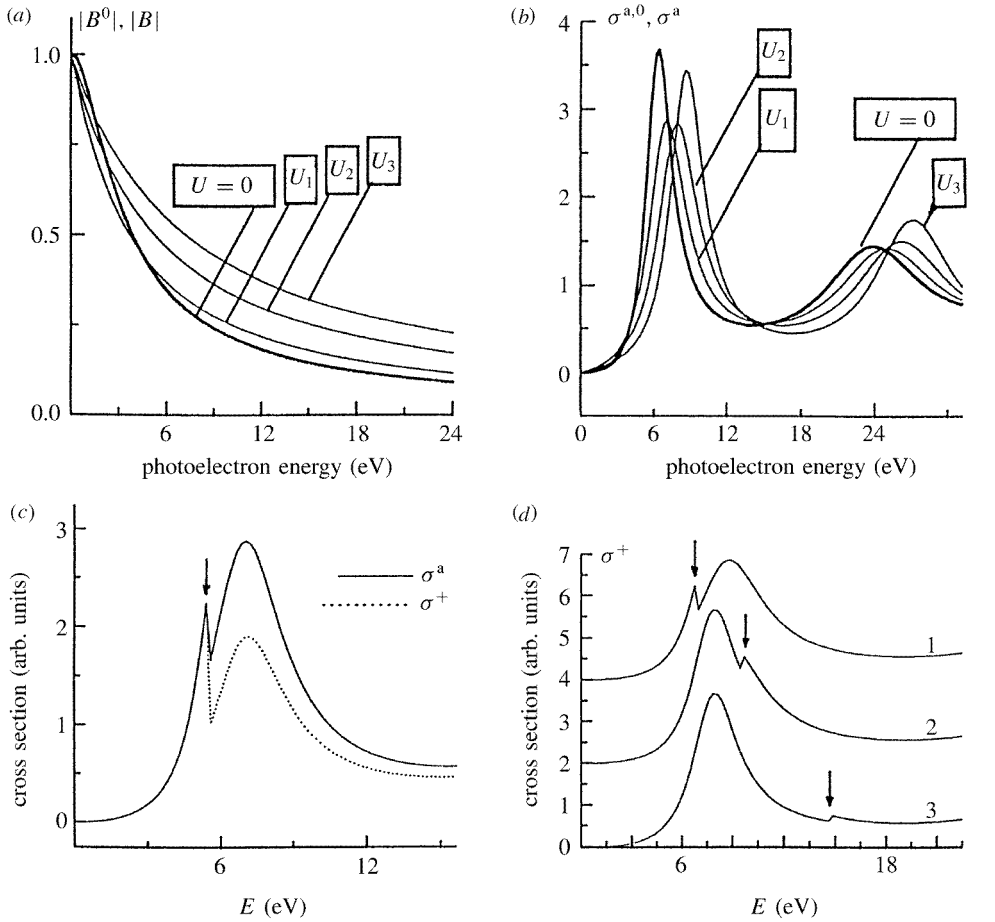

Figure 2. Model spectral dependences of the $|B|$ amplitude and σ^a and σ^+ cross sections as a function of photoelectron losses in the surroundings. (*a*) $|B|$, (*b*) σ^a, ($|B^0|$ and $\sigma^{a,0}$ are shown with bold lines); $0 < U_1 < U_2 < U_3$. (*c*) Shape resonance profile in σ^a and σ^+ at an IT ($\varepsilon = 6$ eV) and (*d*) $\sigma^+(E)$ as a function of IT position (↓).

in both the absorption and ionization spectra much more effectively if ε lies close to the energy E_{SR} of the shape resonance. In the case of weak surroundings for which the $\boldsymbol{B}$ dependence in the right-hand part of equation (6) can be neglected, the breaks come to nil and the exponential damping in equation (11) dominates in the difference between σ^a and σ^+ in accord with equation (1).

The model calculations of the spectral dependence of absorption and single-hole ionization cross sections as a function of the variable imaginary part in the W^{opt} potential show that the U rise leads to (a) the decrease of σ^+ in comparison with σ^a, (b) the upward shifts (e^a and e^+) of the shape resonance position in both spectra and (c) the complicated variation of shape resonance intensity. Even if the imaginary part gives the main contribution to the optical potential, the shape resonance in σ^a stays clearly identifiable, but the shape resonance in σ^+ drops quickly and may disappear. From equations (2) and (3) it follows that

$$\sigma^+(k) \approx e^{-x}\Lambda(z, Z)\,\sigma^a(k) \tag{11}$$

where $\Lambda = \left(1 + z^2 Z\right)\left[Z\left(1 + z^2\right)\right]^{-1}$. $\Lambda \to 1$ at $\kappa \to \infty$, $W \to \infty$ and $U \to 0$. The exponential damping of the photoelectron current outside the molecular region dominates the σ^+:σ^{a} ratio. But for low k the Λ function becomes important, sharply reducing the branching ratio as $\Lambda \to 0$ at $k \to 0$.

Thus, in addition to the exponential decrease of the single-hole ionization cross section relative to that of absorption, extrinsic photoelectron losses lead to anomalous behaviour of both cross sections at IT and the upward shift of the shape resonance energy.

3. C K-shell photoexcitation of CO

3.1. QA calculations

The spectral dependence of C K-shell absorption and single-hole ionization of CO at parallel transitions (σ-channel) in the vicinity of the shape resonance is studied within the framework of the model described above. As O 2p-orbitals play a dominant role in the upper valence shells the low-energy electron impact excitations of CO can be taken approximately for the surroundings excitations. Then, equations (2)–(7) with the $U(E)$ potential determined by using the electron impact cross sections of CO [24, 25] are applicable for the description of the $\sigma^{\mathrm{a}}_{\mathrm{C\,1s}}$ and $\sigma^{+}_{\mathrm{C\,1s}}$ cross sections taking account of the extra-atomic DKO process. At the level of this semi-empirical approach to C K photoexcitation the effect of the C 1s hole on outer shells is not taken into account. Thus, this approach gives the possibility to examine the DKO effect on the spectral dependence taken separately from the C 1s vacancy effect and to bridge the corresponding variations of the C K-shell absorption and single-hole ionization with the electron impact excitation of metastable CO states studied in detail in [24–28].

The calculated spectral dependences of C K photoexcitation of CO are plotted in figure 3. Curve 1 exhibits two coincident dependences of absorption $\sigma^{\mathrm{a},0}_{\mathrm{C\,1s}}$ and single-hole ionization $\sigma^{+,0}_{\mathrm{C\,1s}}$ found without multi-electron excitations. Curves 2 and 3 display the spectral dependences of $\sigma^{\mathrm{a}}_{\mathrm{C\,1s}}$ and $\sigma^{+}_{\mathrm{C\,1s}}$, calculated taking into account the DKO process, but without the satellite excitations due to the C 1s hole creation. The comparison of curves 1–3 demonstrates the appearance of a different spectral dependence of these cross sections and highlights the DKO effect on C K photoexcitation. All curves in figure 3 coincide with each other at $E < 6$ eV, but differ strongly for higher energies. The extrinsic photoelectron losses result in (a) shifts of ≈ 2.3 eV of the shape resonance in $\sigma^{\mathrm{a}}_{\mathrm{C\,1s}}(E)$ and $\sigma^{+}_{\mathrm{C\,1s}}(E)$ to higher E, (b) the decrease of the $\sigma^{+}_{\mathrm{C\,1s}}(E)$ in comparison with $\sigma^{\mathrm{a}}_{\mathrm{C\,1s}}(E)$ and (c) the appearance of new spectral features— a sharp gap labelled ‘a’ at 6 eV and a weak maximum ‘b’ at 10 eV—in both cross sections.

The characteristic feature ‘a’ attracts our main attention as its observation allows us to verify most clearly the predicted DKO effect on the C K-shell photoexcitation. Let us consider its origin. The current of trapped electrons by a CO molecule shows on two well resolved intense maxima at 6 and 10 eV assigned by Mazeau *et al* [26] to transitions from ground $\mathrm{X}\,^1\Sigma^+$ to excited $\mathrm{a}\,^3\Pi$ and $\mathrm{b}\,^3\Sigma^+$ molecular states, respectively. The electron impact excitation cross section for all metastable states of CO starts sharply at 6 eV [24, 25]. The $\mathrm{a}\,^3\Pi$ state with equilibrium geometry close to that of the ground state and well separated from all other states, gives the dominant contribution to the total metastable cross section. As a reference, potential curves of different electronic states of the CO molecule taken from the work [28] are inserted in figure 3. On this background the ‘a’ feature in the $\sigma^{\mathrm{a}}_{\mathrm{C\,1s}}$ and $\sigma^{+}_{\mathrm{C\,1s}}$ cross sections is attributed to the IT behaviour discussed above. It is the coupling of the ground state with the

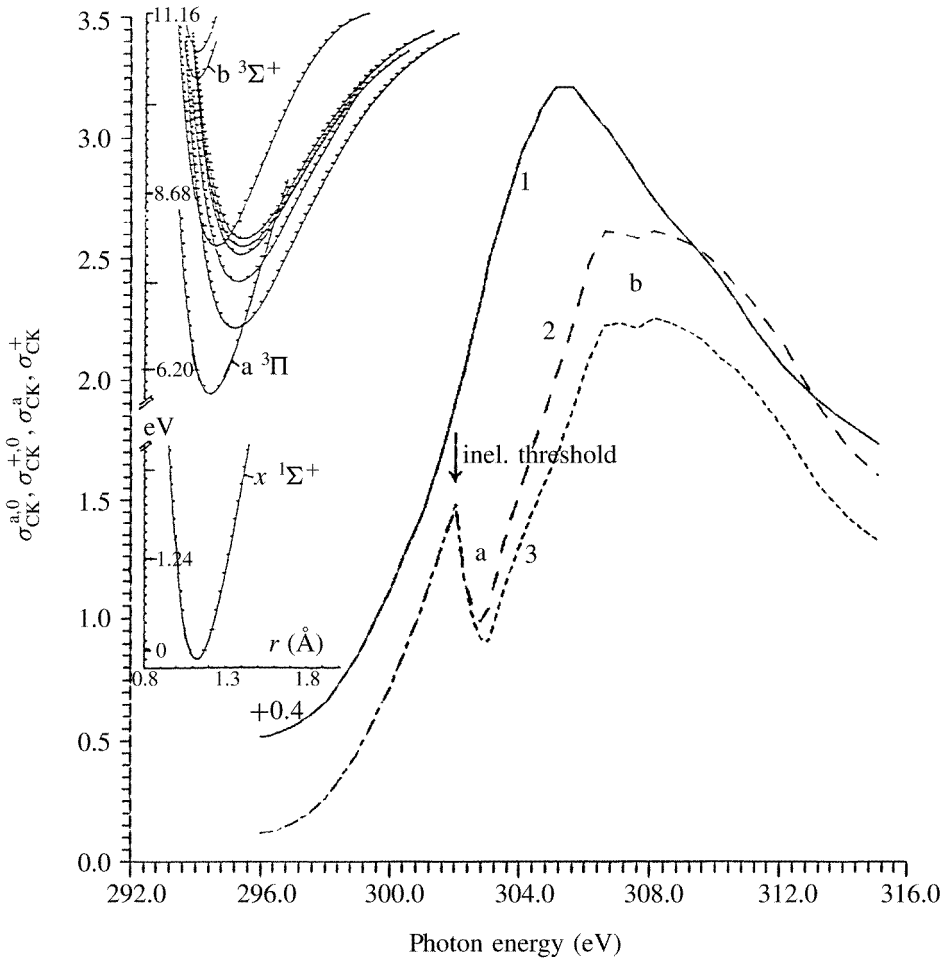

Figure 3. Shape resonances in C K-shell absorption and single-hole ionization spectra of CO. Calculations: 1, $\sigma^{a,0}_{C\,1s}$ and $\sigma^{+,0}_{C\,1s}$; 2, $\sigma^{a}_{C\,1s}$; 3, $\sigma^{+}_{C\,1s}$. Spectra are given on a photon energy scale with $E_{C\,1s} = 296.08$ eV [11]. Inset, some electronic states of the CO molecule produced from data given in [29]).

a $^3\Pi$ state that causes the feature. Taking into account that the C K-shell ionization potential $E_{C\,1s} = 296.08$ eV [1] and $\varepsilon \approx 6.0$ eV (the energy of the X $^1\Sigma^+ \rightarrow$ a $^3\Pi$ transition) the 'a' feature is expected to lie at $\omega_\varepsilon \approx 302$ eV. The spectral variations in the $\sigma^{a}_{C\,1s}$ and $\sigma^{+}_{C\,1s}$ cross sections at higher E are caused by the broad maximum of excitation of all metastable states at ≈ 9 eV [24, 25] and a sharp peak at $\approx$10 eV assigned in the work [24] to the selected excitation of the b $^3\Sigma^+$ state.

3.2. Experimental data analyses

The experimental C K-shell single-hole ionization and absorption cross sections of CO [5] are plotted in figures 4(*a*) and (*b*). The resemblance of the drastic variation of $\sigma^{+,exp}_{C\,1s}(\omega)$ in the interval 300–303 eV in figure 4(*a*) with the calculated spectral dependence of $\sigma^{+}_{C\,1s}$ is seen

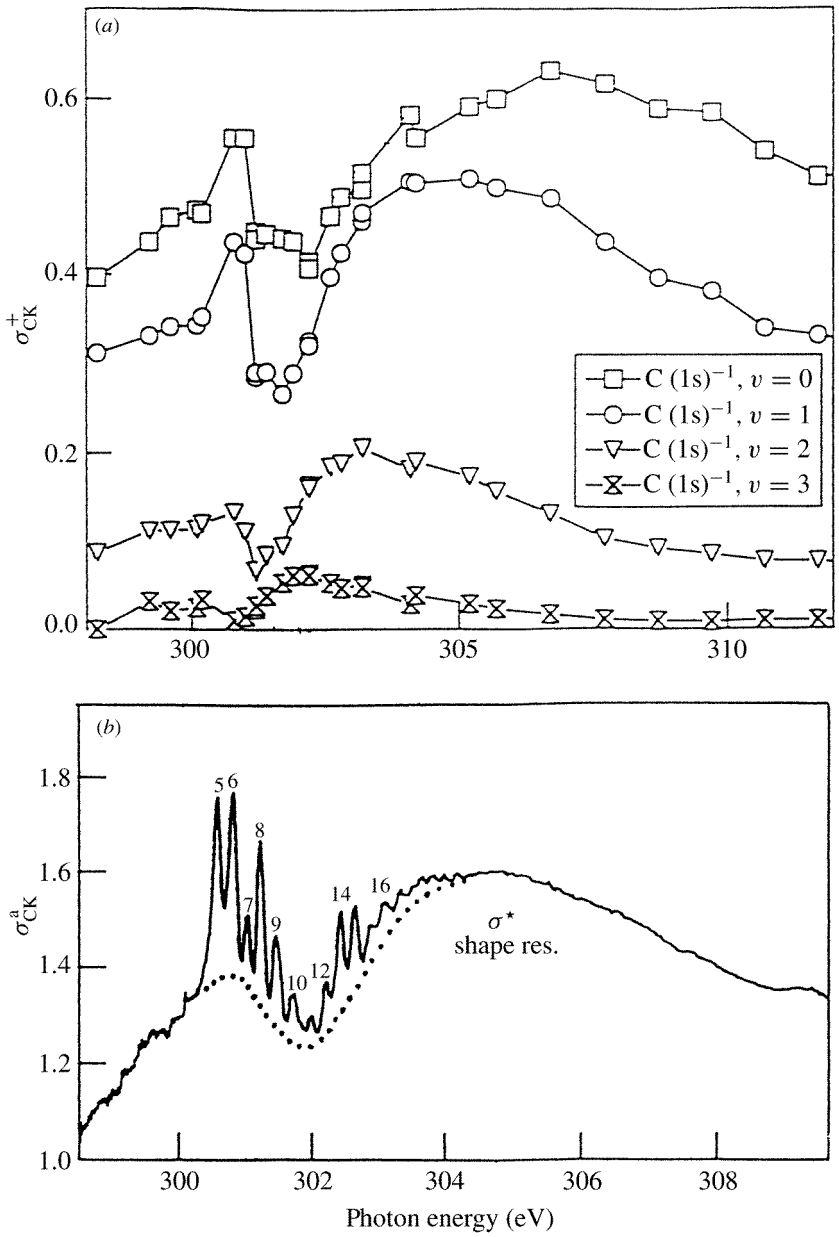

Figure 4. Experimental single-hole ionization cross sections for different vibrational states (*a*) and absorption (*b*) measured in the work [5]. The background of the satellite excitations is shown by a dotted curve.

clearly. The difference (∼1 eV) between the measured position of the gap and calculated ω_ε frequency of the 'a' feature is explained by the effect of the C 1s vacancy on the energy of the $X\,^1\Sigma^+ \rightarrow a\,^3\Pi$ molecular transition. The gap staying practically constant for all vibrational final states (v) [5] supports our assignment of its origin to the IT behaviour. The small energy

shift of the gap to lower ω with increasing v can be assigned to the molecular transition from high vibrational states.

The IT behaviour of the shape resonance in C K-shell absorption of CO was predicted in [30]. But a large contribution of satellite excitations to the $\sigma^{\mathrm{a,exp}}_{\mathrm{C\ 1s}}(\omega)$ discussed earlier in [31] obstructs the observation of the IT feature. The shake up, shake off and double 2e–2h excitations generated by the creation of the core hole lead to the intrinsic photoelectron losses. Their importance at 300–310 eV is seen clearly from the high-resolution electron yield spectrum of CO [5] shown in figure 4(*b*). The intrinsic losses influence the intramolecular interference of photoelectrons inside the surroundings, but should be much weaker than extrinsic ones. Neglecting their coupling one can write $\sigma^{\mathrm{a,exp}}_{\mathrm{C\ 1s}}(\omega) \approx \sigma^{\mathrm{a}}_{\mathrm{C\ 1s}}(\omega) + \sigma_{\mathrm{satellites}}$. Then, curve 2 in figure 3 taken for the background of the satellite excitations demonstrates the close resemblance with the characteristic behaviour of the experimental background in the range 300–303 eV marked by the dotted curve in figure 4(*b*). This provides evidence for the essential DKO effect on the C K-shell absorption cross section. Inspecting the symmetry-resolved C K-shell absorption spectra of the CO molecule [32], a maximum at 302 eV built up from the mixture of non-totally resolved satellite peaks for perpendicular transitions and a minimum at the same energy for parallel transitions are observed. These spectra highlight the different origin of the extrema at 302 eV in the Π and Σ channels. The satellites are mainly accumulated in the Π channel, whereas the spectral dependence in the Σ channel indicates the IT-like behaviour. This difference can be easily explained as the DKO process occurs much more effectively for photoelectrons directed along the molecular axis.

The analysis [5] of the fine structure of photoelectron lines corresponding to the different doubly excited states at transitions from the range ≈ 301 eV to the range ≈ 302 eV demonstrates the population of high vibrational levels with molecular vibrations of smaller frequency. The relevant changes are explainable if one were to include the assistance of the $a\,^3\Pi$ state with a larger equilibrium internuclear distance and a smaller vibration frequency [25] in molecular dynamics of excited states at 302 eV. Furthermore, our analysis of the experimental single C $1s^{-1}$ hole partial cross sections with respect to the model studies (section 2) have shown that the PEVE correlations responsible for the inclusion are minimal for the final states with $v = 0$ and increase for higher vibrational levels. The study [33] of Auger decay spectra from the core-ionized C $1s^{-1}$ state of CO at the shape resonance supports this conclusion. However, in the range ≈ 300–304 eV the $\sigma^{+,\mathrm{exp}}_{\mathrm{C\ 1s}}$ cross section is enhanced by doubly excited C $1s^{-1}\mathrm{Val}^{-1}\pi^{*1}\mathrm{Ryd}^{1}$ states, which autoionize into the C $1s^{-1}$ continuum [5]. The autoionization current is not strong as the profiles of the doubly excited peaks do not indicate a noticeable coupling with the continuum. But the uncertainty in its value makes impossible a precise application of the model calculations to the experimental data for the determination of dynamic characteristics of the molecular excitations.

4. Conclusion and final remarks

Inelastic scattering of the primary photoelectron by valence electrons resulting in their excitation and emission causes the damping of the photoelectron current and the additional phase shift of the photoelectron wave. Due to this phase shift the moving of the photoelectron has to be regarded as correlated by valence excitations. The PEVE correlations change the spectral dependence of the x-ray absorption and single-hole ionization cross sections. The calculations of the C K-shell absorption and single-hole ionization of CO, taking into account the DKO of the valence electrons but ignoring the core-hole effect on them, have demonstrated the important role of the correlations. In comparison with the absorption cross section the

single-hole ionization cross section drops right above the IT, the shape resonance in both spectra shifts to higher energies $E_{SR} - E^0_{SR} = e$ where $e \approx 2.3$ eV, and both cross sections behave irregularly at $\omega_\varepsilon \approx 302$ eV. Based on the resemblance of the C K-shell DKO process to electron-impact excitation of CO it is shown that these spectral changes originate from the essential contribution of the metastable $a\,^3\Pi$ molecular state to C K photoexcitation at the shape resonance. The comparison of the experimental [5] and calculated spectra supports the important role of the PEVE correlations in C K-shell photoexcitation of CO. The present method predicts a drastic variation in both absorption and single-hole ionization spectra at 301–303 eV, providing clear evidence of the correlations. But it does not allow us to reproduce the fine structure in the experimental spectra originating from the C 1s-hole effect on the valence shells. The broad variation in the vicinity of 301–302 eV is interpreted as an IT behaviour of both cross sections due to the $X\,^1\Sigma^+ \rightarrow a\,^3\Pi$ molecular transition induced by DKO of valence electrons by the photoelectron.

In spite of the valence excitations at the IT being very strong, a one-electron description enables us to estimate the C K-shell absorption cross section reasonably. To understand this 'contradiction' let us take into account that the IT lies below the shape resonance, therefore the DKO of valence electrons results in a gap in the absorption and single-hole ionization cross sections. The satellite excitations will smooth the gap in absorption. Thus, the total effect of the photoelectron and the core hole on valence shells indicates the cancellation of extrinsic and intrinsic losses in x-ray absorption fine structure [34–36]. This cancellation disappears if $\varepsilon > E_{SR}$ as both the intrinsic and extrinsic losses give rise to the $\sigma^a(\omega)$ cross section.

The PEVE correlations are expected to influence the angular dependence of C K photoexcitation. Since the DKO of valence shells is maximal for photoelectrons directed along the C–O axis, the PEVE correlations can be associated with repulsion between the photoelectron in the Σ-channel and electrons occupying the 5σ MO. Taking the configuration $1\sigma^2 2\sigma^2 3\sigma^2 4\sigma^2 5\sigma^1 1\pi^4 2\pi^1$ of the $a\,^3\Pi$ state [37] into account, one can see that moving the photoelectron through the molecular region provokes the $5\sigma^{-1}2\pi$ excitation. The $a\,^3\Pi$ state, having a large electric dipole momentum of 1.38 D [24], favours the spd-hybridization which controls the angular distribution of the photoelectrons [2, 8]. Besides, the transfer of angular momentum to the residual molecular ion will provoke essential changes in the angular distribution of the emitted electrons.

The important role of the PEVE correlations in understanding the shape resonance energy–bond-length correlations in chemical compounds could be mentioned. The shape resonance occurring at 305 eV in the photoabsorption spectrum [5] is also present in $\sigma^{+,\mathrm{exp}}_{\mathrm{C\ 1s}}(\omega)$, but its energy shifts from $\approx$307 eV for $v = 0$ to $\approx$302 eV for $v = 3$. This downward shift of the E_{SR} energy for high vibrational levels is not surprising. From the QA view [13], the shape resonance approaches the $1s^{-1}\pi^*$ resonance and they both convert to a C $1s^{-1}2p$ resonance with increasing R_{CO} distance. Determining the $\delta R_{C–O}$ for different v levels in the potential curve for the $X\,^1\Sigma^+$ state [25], the $\partial E_{SR}/\partial R_{C–O}$ derivative is found to be approximately three times larger than the slope κ_{CO} of the linear function $E_{SR}(l_{CO})$, giving the energy position of the shape resonance on C–O bond lengths in the series of chemical compounds [38]. Even if the e shift of the shape resonance is taken into account, the $\partial E_{SR}/\partial R_{C–O}$ and κ_{CO} values describe the essentially different $E_{SR}(R_{CO})$ and $E_{SR}(l_{CO})$ dependences. The $E_{SR}(l_{CO})$ dependence is caused mainly by changes in electron density distribution characterizing C–O bonding in the series of compounds. In contrast to this dependence, chemical effects come to nil for the $E_{SR}(R_{CO})$. It is important for both dependences that the E_{SR} value cannot be assigned to the equilibrium R_{CO} distance of the ground electronic state. Due to the coupling with other metastable states the E_{SR} value must be regarded as a function of two (or more) equilibrium distances: $E_{SR} \approx f\left(R^X_{CO}, R^a_{CO}\right)$ referring to the $X\,^1\Sigma^+$ and $a\,^3\Pi$ molecular states. It is

suitable to mention here that the PEVE correlations may also help explain the C $1s^{-1}$ shape resonances' disappearance in single-hole ionization spectra of the hydrocarbons C_2H_n reported in [7].

Acknowledgment

This work has been supported by the Russian Fund for Basic Investigations (grant no 98-03-32715)

References

[1] Domke M, Xue C, Puschmann A, Mandel T, Hudson E, Shirley D A and Kaindl G 1990 *Chem. Phys. Lett.* **173** 122
[2] Watanabe N, Adachi J, Soejima K, Shigemasa E, Yagishita A, Fominykh N G and Pavlychev A A 1997 *Phys. Rev. Lett.* **78** 4910
[3] Kivimäki A, Kempgens B, Maier K, Köppe H M, Piancastelli M N, Neeb M and Bradshaw A M 1997 *Phys. Rev. Lett.* **79** 998
[4] Schmidbauer M, Kilcoyne A L D, Köppe H-M, Feldhaus J and Bradshaw A M 1992 *Chem. Phys. Lett.* **199** 119
[5] Köppe H M, Kempgens B, Kilcoyne A L D, Feldhaus J and Bradshaw A M 1996 *Chem. Phys. Lett.* **260** 223
[6] Köppe H M, Kilcoyne A L D, Feldhaus J and Bradshaw A M 1995 *J. Electron Spectrosc. Relat. Phenom.* **75** 97
[7] Kempgens B, Köppe H M, Kivimäki A, Neeb M, Maier K, Hergenhahn U and Bradshaw A M 1997 *Phys. Rev. Lett.* **79** 35
[8] Pavlychev A A, Fominykh N G, Watanabe N, Soejima K, Shigemasa E and Yagishita A 1998 *Phys. Rev. Lett.* **81** 3623
[9] Haack N, Ceballos G, Wende H, Srivastava P, Wilhelm F, Ney A, Chauvistre R and Baberschke K 1997 *BESSY, Annual Report* p 334
[10] Stohr J 1992 *NEXAFS Spectroscopy* (*Springer Series in Surface Science* vol 25) (New York: Springer)
[11] Rehr J J, Albers R C and Zabinski S I 1992 *Phys. Rev. Lett.* **69** 3397
[12] Amusia M Ya 1996 *X-Ray and Inner-Shell Processes (Proc. 17th Int. Conf. (Hamburg))* ed R L Johnson, H Schmidt-Bocking and B F Sonntag (New York: AIP) p 389
[13] Amusia M Ya, Chernysheva L V, Gribakin G F and Tsemekhman K L 1990 *J. Phys. B: At. Mol. Opt. Phys.* **23** 393
[14] Amusia M Ya, Gribakin G F and Tsemekhman K L 1989 *Izv. Akad. Nauk SSSR Ser. Fiz.* **53** 1672 (in Russian)
[15] Lee P A, Citrin P H, Eisenberger P and Kincaid B M 1981 *Rev. Mod. Phys.* **53** 769
[16] Fonda L 1992 *J. Phys.: Condens. Matter* **4** 8269
[17] Pavlychev A A, Vinogradov A S, Stepanov A P and Shulakov A S 1993 *Opt. Spektrosk.* **75** 554
Pavlycher A A, Hallmeier K-H, Hennig C, Hennig L and Szargan R 1995 *Chem. Phys.* **201** 547
[18] Pavlychev A A and Fominykh N G 1996 *J. Phys.: Condens. Matter* **8** 2305
[19] Amusia M Ya 1993 *Vacuum Ultraviolet Radiation Physics (Proc. 10th VUV Conf. (Paris, 1992))* ed F J Wuilleumier, Y Petroff and I Nenner (Singapore: World Scientific)
[20] Wu T-U and Ohmura T 1962 *Quantum Theory of Scattering* (New York: Prentice-Hall)
[21] Dernkov Yu N and Ostrovskii V N 1974 *Zero-Range Potential Approximation in Atomic Physics* (Leningrad: Leningrad State University Publishing)
[22] Baz A I 1959 *Adv. Phys.* **8** 349
[23] Breit G 1959 Theory of resonance reactions and applied topics *Handbuch der Physik Herausgegeben* vol XLI, ed S von Flugge, section 1 (Berlin: Springer)
[24] Newman D C, Zubek M and King G C 1983 *J. Phys. B: At. Mol. Phys.* **16** 2263
[25] Morgan L A and Tennyson J 1993 *J. Phys. B: At. Mol. Opt. Phys.* **26** 2428
[26] Reinhardt J, Joyez G, Mazeau J and Hall R I 1972 *J. Phys. B: At. Mol. Phys.* **5** 1884
[27] Le Chair L R and Brown M O 1994 *Chem. Phys.* **180** 769
[28] Mason N J and Newell W R 1988 *J. Phys. B: At. Mol. Opt. Phys.* **21** 1293
[29] Tilford S G and Simmons J D 1972 *J. Phys. Chem. Ref. Data* **1** 147
[30] Pavlychev A A and Davydova G Yu 1993 *Proc. X-93 Conf. on X-Ray and Inner-Shell Processes (Hungary)* Pc 24, p 212
[31] Hitchcock A P and Brion C E 1980 *J. EIectron Spectrosc. Relat. Phenom.* **18** 1
[32] Shigemasa E, Hayashi T, Sasaki T and Yagishita A 1993 *Phys. Rev.* A **47** 1824

[33] Sundin S, Ausmees A, Bjorneholm O, Sorensen S L, Wiklund M, Kikas A and Svensson S 1998 *Phys. Rev.* A **58** 2037
[34] Rehr J J, Bardyszewski W and Hedin L 1997 *J. Physique IV* **7** C2–97
[35] Hedin L 1989 *Physica* B **158** 344
[36] Hedin L 1990 *J. Electron Spectrosc. Relat. Phenom.* **51** 91
[37] O'Neil S V and Schaefer H F III 1970 *J. Chem. Phys.* **53** 3994
[38] Newbury D C, Ishii I and Hitchcock A P 1986 *Can. J. Chem.* **64** 1145